J. Min. Metall. Sect. B-Metall. 49 (3) B (2013) 293 - 297

Journal of Mining and Metallurgy, Section B: Metallurgy

ANALYSIS OF THE MICROSTRUCTURAL EVOLUTION AND SOLIDIFICATION BEHAVIOUR OF Sn-9 wt% Zn ALLOY WITH SMALL ADDITIONS OF Mg

I.A. Figueroa[a], O. Novelo-Peralta[a,*], M.A. Suárez[a], G.A. Lara-Rodríguez[a]

[a] Instituto de Investigaciones en Materiales, Universidad Nacional Autónoma de México, Coyoacán, México

(Received 21 March 2012; accepted 26 June 2013)

Abstract

The microstructure, solidification behaviour and hardness of Sn-9Zn-xMg (where x = 0, 0.5, 2.5 and 5 wt%) alloys were studied. The addition of 0.5 wt% did show a clear effect on the microstructure, producing three distinctive zones: a) fine eutectic structure b) coarse eutectic structure composed by large needles of Zn dispersed into a β-Sn matrix and c) small particles of the intermetallic Mg_2Sn. Further additions of Mg provoked that the fine eutectic structure disappeared, giving place to the formation a coarse eutectic structure, large particles of Mg_2Sn and Zn-rich needles. The hardness of the alloys increased with the additions of Mg. Similarly, the additions of Mg steadily drop the eutectic temperature, from 196.5ºC for the binary base alloy to 180ºC for the alloy with 5 wt% Mg. The low temperature achieved in this alloy is very close to the eutectic Sn-Pb alloy (183ºC), thus it could be a plausible substitute of the classical Pb-containing solder alloys.

Keywords: *Alloys; Solidification; Microstructure, Scanning electron microscopy (SEM)*

1. Introduction

The Waste Electrical and Electronic Equipment (WEEE) and the directive on the Restriction of the Use of Hazardous Substances in Electrical and Electronic Equipment (RoHS Directive) [1–3], have pointed out the urgent necessity for more appropriate substitutes for the traditional Sn–Pb alloys. According to Zhang *et al.* [4] the investigation of Pb-free solder is nowadays one of the most important projects on development and research in this field. They mentioned in their review, that the Sn–Zn solder system could be a candidate for the substitution of Pb-free solder, due to Zn is easily available with low cost [6, 9] and the melting temperature [5-8] of the alloy (198°C) is close to that of Sn–Pb eutectic solder (183°C), when compared with other Sn-based eutectic alloys, for instance: Sn–Cu with 227°C, Sn–Ag with 221°C, Sn–Ag–Cu with 217°C [9]. It is worth mentioning that finding low temperature alloys, would allow the actual use of the current reflow process and apparatus. The main objective when producing new alloys, in order to substitute the Sn–Pb solders, is to ensure that the physical and mechanical properties of these new alloys are comparable or even superior to those alloys that are going to be substituted. However, despite of these characteristics, the tendency for: a) low oxidation-corrosion resistance, b) the poor wettability and c) the relatively high melting point of this alloy have limited its possible applications [10, 11]. From these main characteristics, the melting temperature is critical in any solder, since it determines the maximum operating temperature of the system and the minimum processing temperature that the components, during its working live, must survive [12]. On this basis, there have been a number of alloys [4, 13] that have been reported in the literature with melting points oscillating between 196ºC and 200ºC, this range of temperatures is considered high when compared with the eutectic Sn–Pb solder (183°C). From the above, the objectives of the present work were to study the effect of small addition of Mg on the microstructure of the eutectic Sn-9Zn (wt%) alloy, the influence over the solidification behaviour and the mechanical properties (hardness) of the resultant alloys.

2. Experimental

The general chemical composition of the alloys studied was Sn-9Zn-xMg (where x = 0, 0.5, 2.5 and 5 wt%). The alloys were obtained by melting process using an induction furnace under Argon atmosphere, in order to minimise the loss of Mg by oxidation. The alloy elements were melted in a graphite crucible and were cast in iron moulds. From the ingots produced,

* *Corresponding author: omarnovelo@iim.unam.mx*

DOI:10.2298/JMMB120321031F

several slices were cut and conventional metallographic surface preparation was carried out. The metallographic samples were analysed with a scanning electron microscope (SEM) Leica-Cambridge Stereoscan 440 in order to observe the phases presented in the compositions studied. These observations were supported with X-ray diffraction (XRD) analysis, using a Bruker AXS model D8 Advanced diffractometer, with Cu Kα radiation and a graphite monochromator, operated at 35kV. The cooling curves were obtained by inserting a K-type thermocouple into 100g of the molten alloys, placed in a stainless steel crucible. The alloys were heated up to 300ºC on electric heater prior to the cooling curve measurement. Rockwell R hardness was employed to determine the bulk hardness of the alloys.

3. Results and discussion

3.1. Microstructural characterisation

Figure 1 shows the XRD patterns of binary eutectic Sn-9 wt% Zn alloy together with the alloys with the small additions of Mg. From this figure, in the case of the binary alloy, the existence of the Bragg peaks related to β-Sn and Zn phases of the binary Sn-Zn alloys can be observed. When adding Mg, the reaction with Sn takes place, forming the Mg_2Sn phase. The intensity of Mg_2Sn peaks increases as the Mg content increases, with no other phases detected. This statement is clearly displayed at low angles of the XRD pattern, i.e. between 22.38º and 23º; which corresponds to the planes (1 1 1)Mg_2Sn, according to the JCPDS file with No. 7-274.

SEM analysis was carried out to follow the evolution of the microstructure as the small additions of Mg increased, and to correlate this analysis to the XRD results. Figure 2A shows the microstructure of binary alloy, where a fine homogeneous eutectic structure, composed by small needles corresponding to the Zn phase (black) dispersed into a β-Sn matrix (gray) is clearly observable. This microstructure has already been reported in the literature [13], which confirms the good metallurgical practice during the preparation of the alloys and the reliability of the results presented in this study. The addition of 0.5 wt% of Mg to binary alloy did show a clear effect on the microstructure, as shown in Figure 2B. From this figure, three zones were identified; zone (a) showed a fine eutectic structure, similar to the one shown in Figure 2A, which corresponds, exclusively, to the binary eutectic composition. Zone (b) displayed a coarse eutectic structure composed by large needles of Zn (black) dispersed into a β-Sn matrix (grey). Finally, in zone (c), small particles of the intermetallic Mg_2Sn were observed. These small particles correspond to the evolution of the weak Bragg peaks shown in Figure 1, for the composition with 0.5 wt% of Mg. It is thought that the evolution and growth of the large needles of Zn are due to the consumption of part of Sn of the alloy to form the intermetallic Mg_2Sn, leaving the Zn to growth in such fashion. It is evident, from this figure, that the growth of this intermetallic is located at the boundary of zones (a) and (b). This tells us that the formation of this intermetallic is governed by the depletion of Sn from zone (b) allowing the growth of the coarse Zn structure. As the content of Mg increases the fine eutectic structure disappears and a coarse eutectic

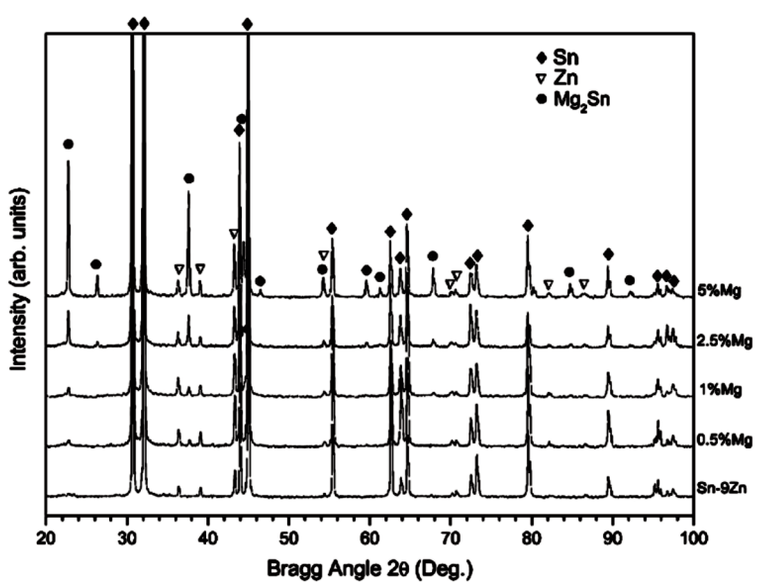

Figure 1. *XRD patterns of the Sn-Zn-xMg (x= 0, 0.5, 1, 2.5 and 5 wt%) alloys*

structure becomes predominant. Figure 2C shows the microstructure of alloy with 2.5 wt% of Mg. In this case, large particles of Mg_2Sn and Zn-rich needles immersed in a coarse eutectic structure, and some small zones of fine eutectic structure were observed. Zone (a) of this figure, shows the remanent of the fine eutectic structure. Zone (b) shows the large particles of the intermetallic Mg_2Sn, these particles grew in such manner that the original prismatic structure changed to an irregular shape, it is thought that the critical size for changing such shape, i.e. from a well-defined prismatic to an irregular semi-prismatic shape, lays between 15 and 20 μm. It is worth noting that these particles did not show a good coherent interface with the matrix, as there were some cracks between them and the matrix, and more importantly, some of them were removed during the polishing. As mentioned above, the large needles of Zn that were developed in the alloy with 2.5 wt% Mg are related to consumption of Sn to form the intermetallic Mg_2Sn, leaving the Zn to growth. On the other hand, since the fine eutectic structure, which is responsible of supplying the Zn, is decreasing considerably, the free Zn free in the alloy has to migrate, provoking the homogeneous growth of these large needles in the alloy structure.

Finally, the SEM micrograph of the alloy with 5 wt% Mg is shown in Figure 2D. The effect of the addition of 5 wt% Mg to the base alloy is rather considerable. The concentration of Mg_2Sn particles did increase, however, the size of such particles was smaller than the particles of this intermetallic observed in the alloy with 2.5 wt% Mg. The Mg_2Sn particles formed at this concentration of Mg showed a more homogeneous shape, size and distribution, but they also had bad coherent interface with the matrix, here, there were also observed some cracks between them and the matrix and a number of particles were removed during the metallographic preparation. These particles were also embedded in the coarse eutectic structure, few large Zn-rich zones were found and, for this composition, the zones that previously showed a fine eutectic structure were not identified.

3.2 solidification behaviour

Figures 3A-3D display the cooling curves of the alloys with the small additions of Mg. In general, the changes in the solidification behaviour as the addition of Mg increased were very noticeable. Figure 3A shows the cooling curve of the binary Sn-9wt%Zn alloy; this curve clearly displays the typical solidification behaviour of a eutectic alloy. In this figure the starting point of the cooling curve plot is

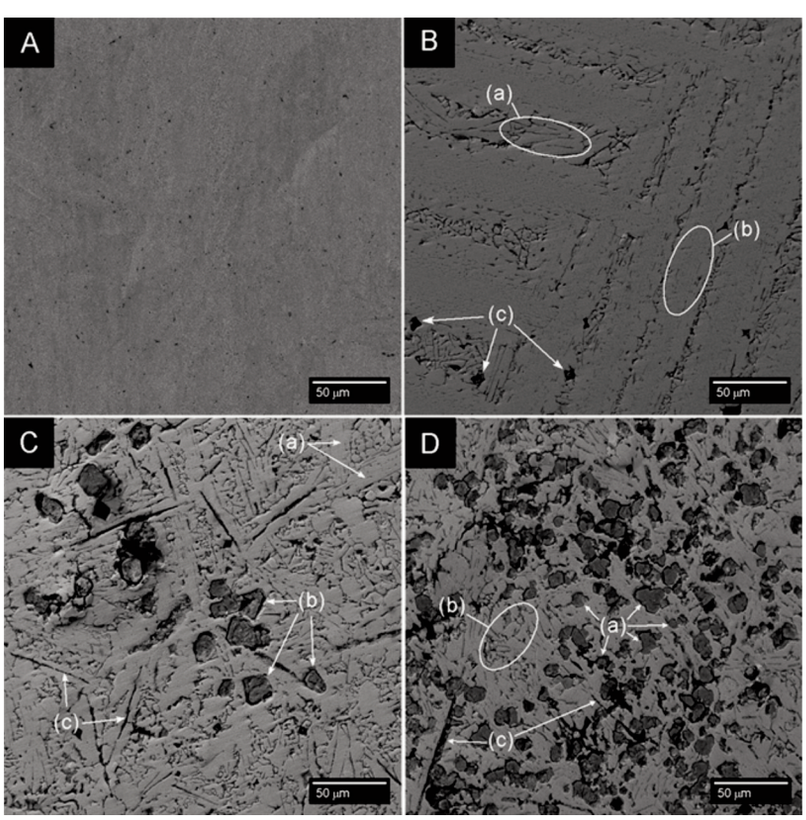

Figure 2. *SEM backscattered electron images of: (A) Binary eutectic alloy Sn-9 wt% Zn; (B) 0.5 wt% Mg; (C) 2.5 wt% Mg and (D) 5 wt% Mg, alloy microstructures*

any temperature of the alloy in liquid state (Segment I-II), in this case the starting point was 270ºC. As time goes by, and there is a phase change, the well-known thermal arrest occurs, here is where the temperature remains constant. The energy required for a phase change is known as latent heat and the cooling rate is the slope of the cooling curve at any point. In the part of the curve where the temperature decreases, the kinetic energy also decreases while the potential energy remains equal. But, at the phase transition, i.e. where the curve turns flat, the kinetic energy stays the same whilst the potential energy drops. In point II, a recalescence effect caused by nucleation phenomena is observed. As mentioned above, the formation of eutectic structure begins in the segment II-III (isothermic segment). This transformation is given at temperature of 196.5ºC following the eutectic reaction $L \rightarrow \beta\text{-Sn} + Zn$, that was reported to occur at 198.5 ºC [14, 15]. Finally, after the liquid alloy completely transforms to solid, begins its cooling to room temperature (segment III-IV). Table 1 shows the cooling rate for the alloys investigated.

As the Mg content is increased from 0.5 to 5wt%, the solidification behaviour changes, significantly, with respect to the binary alloy, as can be observed in Figures 3B-3D. The main change in solidification of these alloys is that the liquid-solid transformation is divided in two segments (II-III and III-IV, respectively). In all cases, a horizontal segment is observed i.e. segment III-IV, which is associated to the ternary eutectic reaction: $L \rightarrow Mg_2Sn + \beta\text{-Sn} + Zn$, and takes place at a temperature of 180ºC, approximately. The reported temperature for ternary eutectic reaction is among 181.5 ºC [15] to 183 ºC [14]. It is though that segment II-III for the alloy with 0.5wt% Mg could be associated to the formation of the fine eutectic structure and the segregation of Zn to form the coarse eutectic, as shown in Figure 2B. As can be seen in the ternary phase diagram reported in ref [14], for 0.5 wt.% the alloy lies between the eutectic and ternary eutectic reactions, resulting in the coexistence of these two microstructures. Finally, segment II-III of the alloys with 2.5 and 5 wt% of Mg is directly associated to the formation of the Zn needles displayed in Figures 2C and 2D, respectively. According to the phase diagram reported in ref [14], for additions of 2.5 and 5 wt.% of Mg, the alloys lie in a region after the ternary

Table 1. *Cooling rates of the alloys investigated*

Alloy	Cooling rate [ºC/s]
Binary (Sn-9 wt% Zn)	1.645
0.5 wt% Mg	1.65
2.5 wt% Mg	1.468
5 wt% Mg	1.189

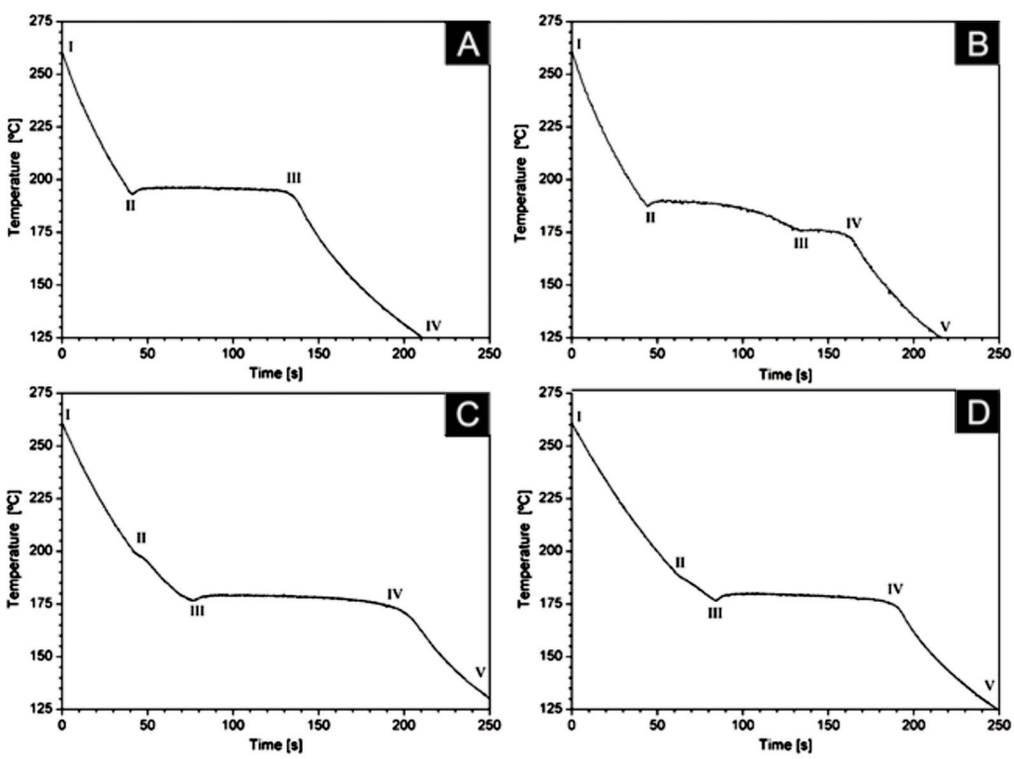

Figure 3. *Cooling curves of: (A) Binary eutectic alloy Sn-9 wt% Zn, (B) 0.5 wt% Mg; (C) 2.5 wt% Mg and (D) 5 wt% Mg, alloys*

eutectic reaction, developing a coarse eutectic microstructure.

3.3. Mechanical properties

Figure 4 displays the behaviour of the Rockwell R hardness (HRR) with the small additions of Mg to the binary Sn-9Zn. This figure shows that the hardness of the base alloy raises as the Mg content increases. The hardness value of the base alloy was 87±4 HRR. However, with the addition of 0.5 wt% Mg the hardness increased up to 104±1 HRR. This increment in hardness could be attributed to the formation of the coarse eutectic structure, since the formation of the coarse eutectic could stop the dislocation movement, promoting the enhancement of hardness of the base alloy. With further additions of Mg, the hardness did increase but not as pronounce as with 0.5wt% Mg, increasing from 106±1 HRR to 111±1 HRR for the alloys with 2.5wt% Mg and 5 wt% Mg, respectively. In these alloys, the coarse eutectic, together with the formation of the intermetallic Mg_2Sn compound and the large Zn-rich needles, acted as further obstacles to the dislocations movement.

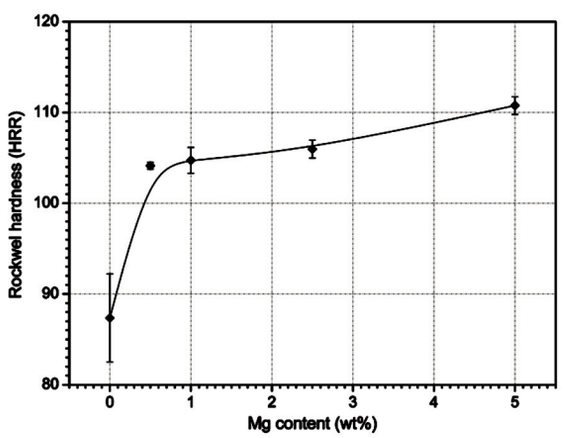

Figure 4. *Evolution of Rockwell hardness as a function of Mg content*

4. Conclusions

The XRD analyses showed that the Mg was easily incorporated into the Sn-Zn structure. The addition of 0.5 wt% of Mg changed the microstructure of the base binary alloy. Three zones were identified; (a) fine eutectic structure, (b) coarse eutectic structure composed by large needles of Zn dispersed into a β-Sn matrix and, (c) small particles of the intermetallic Mg_2Sn. As the Mg content increased, the fine eutectic structure tend to disappear giving place to the formation a coarse eutectic structure, together with the formation of large particles of Mg_2Sn and Zn-rich needles immersed in the above mentioned coarse eutectic. The formation of these phases did have a strong correlation with the resulting mechanical behaviour. The initial increment of hardness was directly associated to the formation of the coarse eutectic and the further increase was related to the mixture of the coarse eutectic, the presence the dispersed Mg_2Sn particles and the formation of large Zn-rich needles in the alloy. From the cooling curves, the addition of Mg drops the eutectic temperature down to 180ºC, giving a difference of 16.5ºC from the binary Sn-Zn alloy (196.5ºC). This temperature is rather close to the eutectic temperature of the Sn-Pb alloy (183ºC); therefore, the aforementioned alloy could be very promising as a plausible substitute of the classical Pb-containing solder alloys.

Acknowledgements

Authors would like to thank to A. Tejeda, G. Aramburo, J. J. Camacho, E. Sanchez, C. González, C. Delgado, G. González and J. Morales for their technical support. IAF also acknowledge the financial support of PAPIIT-UNAM and SEP-CONACyT through grants No. RR180712 and 178289, respectively.

References

[1] J. O. Kim, J. P. Jung, J. H. Lee, J. Suh, H. S. Kang, Met. Mater. Int., 15(1) (2009) 119-123.

[2] L. Zhang, S. B. Xue, Y. Chen, Z. J. Han, J. X. Wang, S. L. Yu, F. Y. Lu, J. Rare Earths, 27(1) (2009) 138-144.

[3] J. B. Pan, B. J. Toleno, T. C. Chou, W. J. Dee, Solder. Surf. Mt. Technol., 18(4) (2006) 48-56.

[4] L. Zhang, S. B. Xue, L. Gao, Z. Sheng, H. Ye, Z. X. Xiao, G. Zeng, Y Chen, S. L. Yu, J. Mater. Sci.: Mater. Electron., 21(1) (2010) 1-15.

[5] M. McCormack, S. Jin, JOM, 45 (1993) 36-40.

[6] M. Abtew, G. Selvaduray, Mater. Sci. Eng. R-Reports, 27(5-6) R (2000) 95-141.

[7] H. Mavoori, J. Chin, S. Vaynman, B. Moran, L. Keer, M. Fine, J. Electron. Mater., 26(7) (1997) 783-790.

[8] K. Suganuma, T. Murata, H. Noguchi, Y. Toyoda, J. Mater. Res., 15(4) (2000) 884-891.

[9] J. Sopousek, J. Vrestal, A. Zemanova, J. Bursi , J. Min. Metall. Sect. B-Metall. 48 (3) B (2012) 419-425.

10] E. P. Wood, K. L. Nimmo, J. Electron. Mater., 23(8) (1994) 709-713.

[11] K. Suganuma, K. Niihara, T. Shoutoku, Y. Nakamura, J. Mater. Res., 13(10) (1998) 2859-2865.

[12] J. Glazer, J. Electron. Mater., 23(8) (1994) 693-700.

[13] K. I. Chen, S. C. Cheng, S. Wu, K. L. Lin, J. Alloys Compd., 416(1-2) (2006) 98-105.

[14] G. Effenberg, S. Ilyenko. Landolt-Börnstein. Group IV: Physical Chemistry. Ternary Alloy Systems Phase Diagrams, Crystallographic and Thermodynamic Data (W. Martienssen). Springer Verlag, Heidelberg-Berlin, 2006, p. 356-365.

[15] P. Ghosh, M. Mezbahul-Islam, M. Medraj, CALPHAD 36 (2012) 28–43.